



# Benzoimidazolium-derived dimeric and hydride n-dopants for organic electron-transport materials: impact of substitution on structures, electrochemistry, and reactivity

Swagat K. Mohapatra<sup>\*1,2</sup>, Khaled Al Kurdi<sup>1</sup>, Samik Jhulki<sup>1</sup>, Georgii Bogdanov<sup>3</sup>, John Bacsa<sup>4</sup>, Maxwell Conte<sup>1</sup>, Tatiana V. Timofeeva<sup>3</sup>, Seth R. Marder<sup>\*1,5,6,7</sup> and Stephen Barlow<sup>\*1,5,7</sup>

## Full Research Paper

[Open Access](#)

### Address:

<sup>1</sup>Center for Organic Photonics and Electronics and School of Chemistry and Biochemistry, Georgia Institute of Technology, Atlanta, GA 80007, United States, <sup>2</sup>Department of Industrial and Engineering Chemistry, Institute of Chemical Technology—Indian Oil Campus, ITT Kharagpur Extension Center, Bhubaneswar 751013 Odisha, India, <sup>3</sup>Department of Chemistry, New Mexico Highlands University, Las Vegas, New Mexico 87701, United States, <sup>4</sup>Crystallography Lab, Emory University, Atlanta, Georgia 30322, United States, <sup>5</sup>Renewable and Sustainable Energy Institute (RASEI), University of Colorado Boulder, Boulder, Colorado 80309, United States, <sup>6</sup>Department of Chemical and Biological Engineering and Department of Chemistry, University of Colorado Boulder, Boulder, Colorado 80309, United States and <sup>7</sup>National Renewable Energy Laboratory, Chemistry and Nanoscience Center, Golden, Colorado, 80401, United States

### Email:

Swagat K. Mohapatra<sup>\*</sup> - sk.mohapatra@iocb.ictmumbai.edu.in;  
Seth R. Marder<sup>\*</sup> - seth.marder@colorado.edu; Stephen Barlow<sup>\*</sup> - stephen.barlow@colorado.edu

\* Corresponding author

### Keywords:

benzoimidazole; crystal structure; kinetics; n-dopant; reduction

Beilstein J. Org. Chem. 2023, 19, 1651–1663.

<https://doi.org/10.3762/bjoc.19.121>

Received: 09 August 2023

Accepted: 17 October 2023

Published: 01 November 2023

This article is part of the thematic issue "Organic electron transport materials".

Associate Editor: P. J. Skabara



© 2023 Mohapatra et al.; licensee Beilstein-Institut.  
License and terms: see end of document.

## Abstract

1,3-Dimethyl-2,3-dihydrobenzo[*d*]imidazoles, **1H**, and 1,1',3,3'-tetramethyl-2,2',3,3'-tetrahydro-2,2'-bibenzo[*d*]imidazoles, **12**, are of interest as n-dopants for organic electron-transport materials. Salts of 2-(4-(dimethylamino)phenyl)-4,7-dimethoxy-, 2-cyclohexyl-4,7-dimethoxy-, and 2-(5-(dimethylamino)thiophen-2-yl)benzo[*d*]imidazolium (**1g-i<sup>+</sup>**, respectively) have been synthesized and reduced with NaBH<sub>4</sub> to **1gH**, **1hH**, and **1iH**, and with Na:Hg to **1g<sub>2</sub>** and **1h<sub>2</sub>**. Their electrochemistry and reactivity were compared to those derived from 2-(4-(dimethylamino)phenyl)- (**1b<sup>+</sup>**) and 2-cyclohexylbenzo[*d*]imidazolium (**1e<sup>+</sup>**) salts.  $E(1^+/1^*)$  values for 2-aryl species are less reducing than for 2-alkyl analogues, i.e., the radicals are stabilized more by aryl groups than the cations, while 4,7-dimethoxy substitution leads to more reducing  $E(1^+/1^*)$  values, as well as cathodic shifts in  $E(1_2^{*+}/1_2)$  and  $E(1H^{*+}/1H)$  values. Both the use of 3,4-dimethoxy and 2-aryl substituents accelerates the reaction of the **1H** species with PC<sub>61</sub>BM. Because 2-aryl groups stabilize radicals, **1b<sub>2</sub>** and **1g<sub>2</sub>** exhibit weaker bonds than **1e<sub>2</sub>** and **1h<sub>2</sub>** and thus react with 6,13-bis(triisopropyl-

silylethynyl)pentacene (**VII**) via a “cleavage-first” pathway, while **1e<sub>2</sub>** and **1h<sub>2</sub>** react only via “electron-transfer-first”. **1h<sub>2</sub>** exhibits the most cathodic  $E(1_2^{•+}/1_2)$  value of the dimers considered here and, therefore, reacts more rapidly than any of the other dimers with **VII** via “electron-transfer-first”. Crystal structures show rather long central C–C bonds for **1b<sub>2</sub>** (1.5899(11) and 1.6194(8) Å) and **1h<sub>2</sub>** (1.6299(13) Å).

## Introduction

Electrical doping of organic semiconductors can play an important role in tuning the properties of organic semiconductors for a variety of applications [1–5]. The most straightforward n-dopants for doping electron-transporting materials are simple one-electron reductants; however, to be effective for a wide range of semiconductors, they must exhibit low ionization energies and thus air sensitivity. One approach to circumvent this issue is to identify systems where the electron-transfer process is coupled to other chemical reactions, increasing the kinetic stability of the dopant to air, and thus increasing its ease of storage and handling.

Arguably, the most widely investigated air-inert n-dopants are 1,3-dimethyl-2,3-dihydrobenzo[*d*]imidazoles (DMBI-H, **1H**, Figure 1); these species have been known for decades (e.g., **1aH**, one of the simplest such derivatives, was first reported in 1954 [6]), but were only introduced in n-dopants in 2010, when Bao and co-workers reported the use of N-DMBI-H (**1bH**, Figure 1) to n-dope fullerenes [7]. Although widely used, due to their facile synthesis, structural tunability, and good air stability in the solid state, **1H** derivatives are relatively limited in dopant strength and their reactivity with organic semiconductors (SC) does not depend solely on the SC reduction potential, since the first step, at least in many cases, is a hydride transfer rather than an electron transfer [8,9]. Moreover, as well forming the desired semiconductor radical anion  $SC^{•-}$ , and the stable  $DMBI^+$  (**1<sup>+</sup>**) species, a hydrogen atom must be lost from the dopant, in some cases resulting in the incorporation of hydrogen-reduced side products into the semiconductor film [9], although in other cases it may be lost as H<sub>2</sub> [8,10,11].

The first report of a (DMBI)<sub>2</sub> dimer (**1<sub>2</sub>**, Figure 1) was of **1a<sub>2</sub>** in 1984 [12]. More recently, dimers **1b<sub>2</sub>–1f<sub>2</sub>** (Figure 1) have been used as n-dopants [13–20]. They behave similarly to the closed-shell dimers formed by certain 19-electron transition-metal sandwich compounds [21–23], exhibiting moderate air stability and acting as quite strong dopants, reacting with semiconductors more rapidly and predictably than hydride donors such as the corresponding **1H** species [8], cleanly only to give  $SC^{•-}$  and the corresponding monomeric cations. However, **1<sub>2</sub>** dopants offer the possibility of more planar dopant ions than the organometallic dimers, which can be advantageous [19].

Although the impact of different 2-aryl Y groups on the reactivity of **1H** species have been examined [9,24], there has been no

direct comparison of the solution reactivity (or doping behavior) of **1H** or **1<sub>2</sub>** reductants with Y = aryl substituents to that of their Y = alkyl counterparts, while there has also been limited effort on examining the effects of substituents on the benzimidazole 6-membered ring in either class of reductant [16,24]. Furthermore, there has been little work on Y = 2-thienyl **1H** derivatives. Here, we report two new dimers (**1g<sub>2</sub>** and **1h<sub>2</sub>**) and three new hydride donors (**1gH**, **1hH**, **1iH**). We also report crystal structures of several of these compounds and of several salts of the corresponding **1<sup>+</sup>** cations, and compare the electrochemistry and reactivity of these species.

## Results and Discussion

### Synthesis

Although an unsymmetrical **1<sub>2</sub>**-like molecule, 2-diethoxyphosphoryl-1,1',3,3'-tetramethyl-2,2',3,3'-tetrahydro-2,2'-bibenzo[*d*]imidazole, has been obtained from addition of HPO<sub>3</sub>Et<sub>2</sub> across the central C=C bond of bis(1,3-dimethylbenzoimidazolinidin-2-ylidene) [25], **1<sub>2</sub>** dimers have generally been obtained by reductive electrochemical or chemical dimerization of **1<sup>+</sup>** cations [12,13,16,19,26]. **1H** derivatives can be obtained in a number of ways, including direct condensation of *N,N'*-dimethylphenylene-1,2-diamine derivatives with the appropriate aldehydes, YCHO [24,27], or borohydride reduction of **1<sup>+</sup>** salts [24]. The cations conversely can be obtained from **1H** derivatives, for example through hydride abstraction by Ph<sub>3</sub>C<sup>+</sup> [13]. Alternatively, they can also be obtained by condensation of *N,N'*-dimethylphenylene-1,2-diamine derivatives with acid chlorides, YCOCl, or through the methylation of 2-substituted benzoimidazoles [24], which in turn can be obtained from condensation between phenylene-1,2-diamines and carboxylic acids YCO<sub>2</sub>H [28], oxidative condensation between YCHO and phenylene-1,2-diamines [29], or reductive condensation between YCHO and 2-nitroanilines [24].

In this work we condensed the appropriate YCHO aldehyde (**II**) and 1,2-diaminobenzene (**I**) derivatives in the presence of sodium metabisulfite (Na<sub>2</sub>S<sub>2</sub>O<sub>5</sub>) [29] to obtain the corresponding substituted benzimidazoles (**III**) in essentially quantitative yield (Scheme 1). In the absence of Na<sub>2</sub>S<sub>2</sub>O<sub>5</sub>, but under otherwise similar conditions, we obtained in some cases the imines in which one of the amino groups condenses with the aldehyde but where the subsequent second condensation and oxidation does not take place, i.e., structures of type **IV** (Scheme 1), which are known to be converted to benzimidazoles by various oxidants

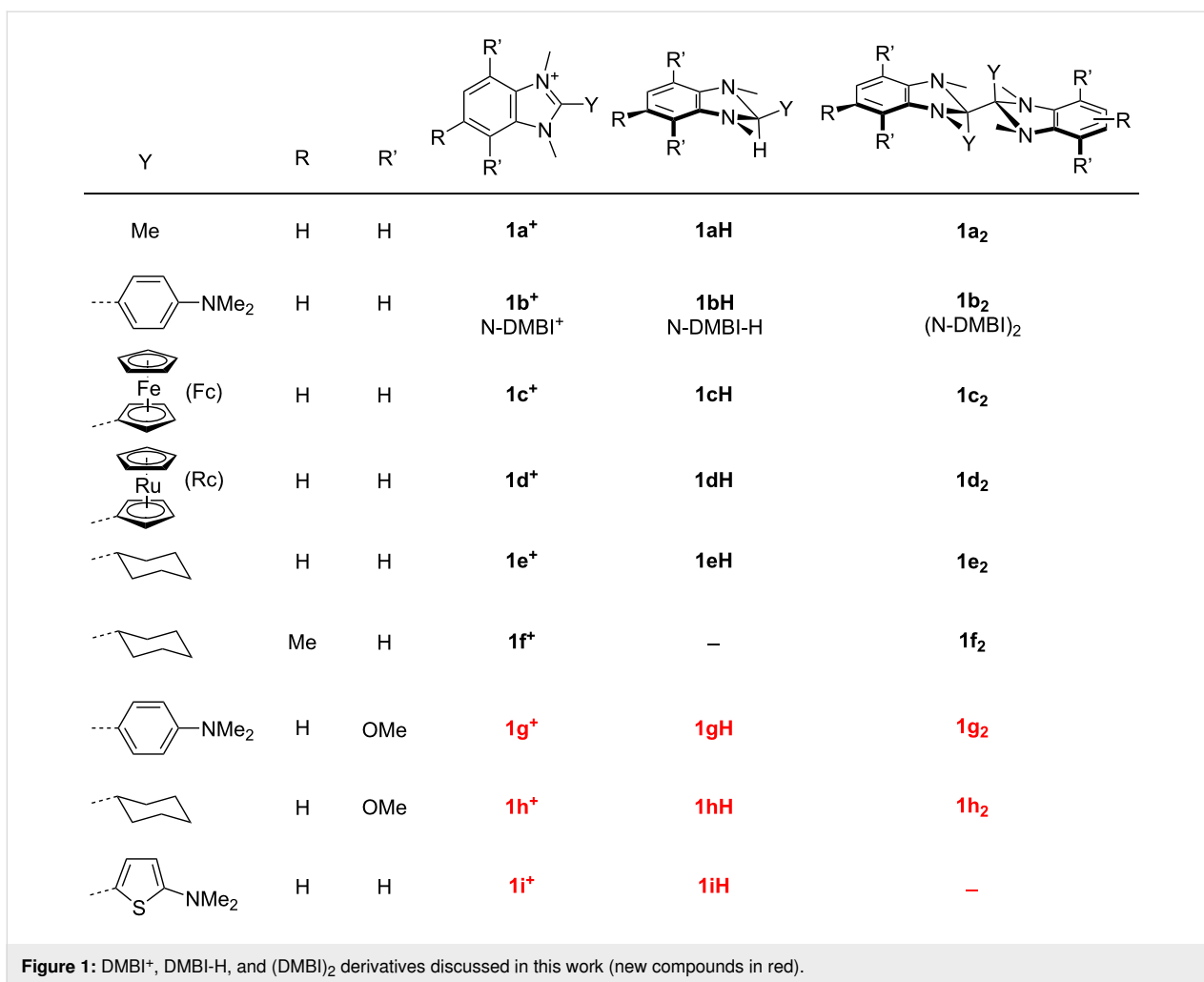
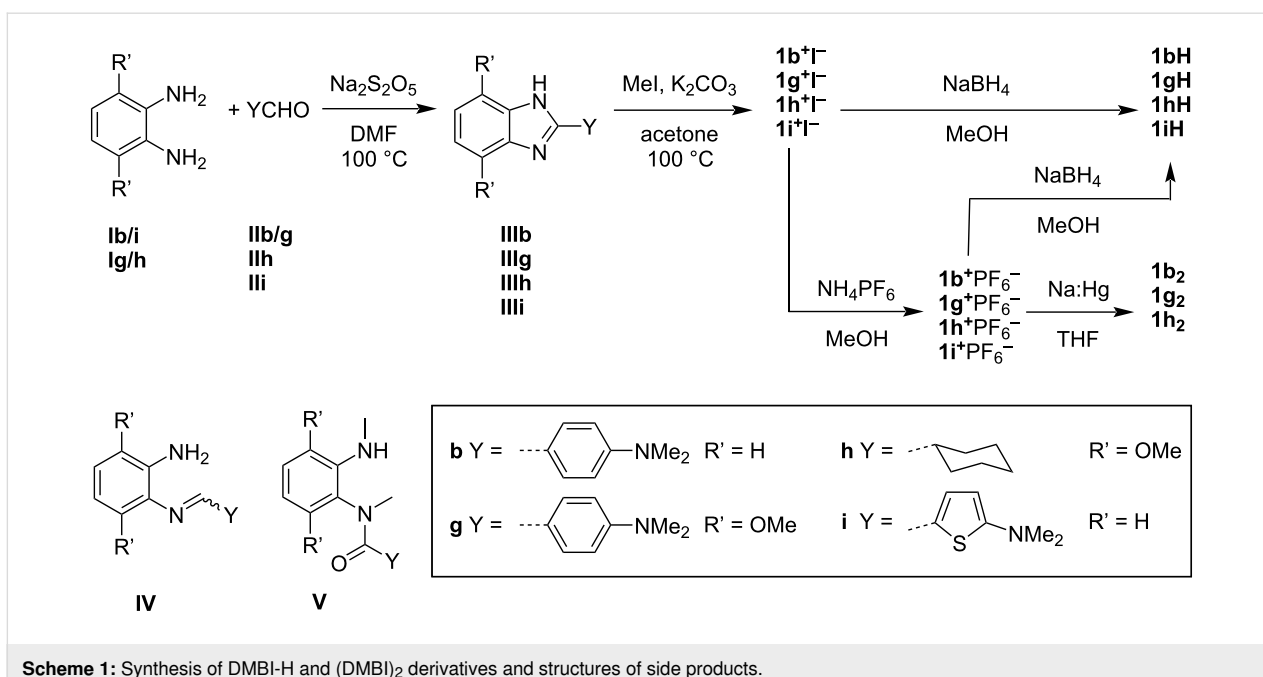


Figure 1: DMBI<sup>+</sup>, DMBI-H, and (DMBI)<sub>2</sub> derivatives discussed in this work (new compounds in red).



Scheme 1: Synthesis of DMBI-H and (DMBI)<sub>2</sub> derivatives and structures of side products.

and/or catalysts [30–32]. The benzimidazoles were then doubly methylated with iodomethane (or methyl tosylate) to afford the benzimidazolium iodides (or tosylates),  $1^+I^-$  (or  $1^+OTs^-$ ), which were metathesized to the corresponding hexafluorophosphates,  $1^+PF_6^-$ . Either  $I^-$  or  $PF_6^-$  salt can then be converted to the corresponding **1H** derivative using  $NaBH_4$  in MeOH. The  $PF_6^-$  salts are somewhat more soluble than the iodides in THF, so were reductively dimerized to **1<sub>2</sub>** in THF using  $Na:Hg$ , although reduction of  $1^+PF_6^-$  failed to afford **1<sub>2</sub>**. As we have noted before for other **1<sub>2</sub>** species, amides (**V**, Scheme 1) are encountered as both byproducts of dimer synthesis and dimer decomposition products [14]. **V** derivatives have also been obtained as pyrolysis products of a variety of  $Y = aryl$  **1H** derivatives [33], while **Vb** has also been found to be both a solution decomposition product of **1bH** [27,34] and a beneficial additive for a **1bH**-doped polymer [27], and has been crystallographically characterized [34]. In the case of molecules with aryl  $Y$ -substituents – **1b<sub>2</sub>** and **1g<sub>2</sub>** – the room-temperature  $^1H$  and  $^{13}C$  NMR spectra (see Supporting Information File 1, Figures S2, S26 and S27, and reference [26]) display more resonances than expected based on the highest symmetry possible for the molecule indicating that the sample represents neither solely a high-symmetry conformer, nor a mixture of rapidly exchanging lower symmetry conformers. In the case of **1b<sub>2</sub>** all the proton resonances are rather broad, and variable-temperature experiments (see Supporting Information File 1, Figure S2) showed further broadening and then coalescence of some of these peaks on increasing the temperature, consistent with the room-temperature spectrum being affected by restricted rotation; interestingly the crystal structure of **1b<sub>2</sub>** contains molecules with two very different conformations (see below).

The **1<sub>2</sub>** dimers are somewhat more sensitive to air than the corresponding **1H** hydrides, but are all sufficiently stable as solids that they can briefly be handled in air, for example, for weighing. The solids do decompose slowly in air, although we

have not quantified this; in inert atmosphere, however, they are completely stable (at least 4 months for solid **1b<sub>2</sub>**). Both **1H** and **1<sub>2</sub>** derivatives decompose more rapidly on exposure to air in solution. In  $CDCl_3$  decomposition is rapid, consistent with the reactivity of many reductants with that solvent. In  $C_6D_6$  these compounds are more stable, allowing, for example, rapid acquisition of a  $^1H$  NMR spectrum; however, handling under nitrogen is advisable as these species completely decompose to **V** (and perhaps  $1^+$  species) on timescales of hours to days (see Supporting Information File 1, Figures S3–S5).

## Crystal structures

We have determined the structures of two **1<sub>2</sub>** dimers, four **1H** derivatives (including **1bH**, the structure of which has previously been reported, but with somewhat lower precision than in the present work [34]), and three salts of  $1^+$  cations using single-crystal X-ray diffraction. Here, we briefly discuss some of the more interesting structural findings; a more detailed comparison of structural parameters is given in the Supporting Information File 1, Table S2. In particular, we are aware of only two previously reported crystal structures of DMBI dimers [14], although several related structures of organic dimers, including those of benzothiazoline, benzoxazoline, acridanyl, morpholinonyl dimers (**2<sub>2</sub>–5<sub>2</sub>**, respectively, Figure 2) have been reported in different chemical contexts [35–38]. The crystal structure of (N-DMBI)<sub>2</sub>, **1b<sub>2</sub>** (Figure 3), contains two crystallographically inequivalent molecules that are geometrically rather different from each other. One of the molecules has crystallographic inversion ( $C_i$ ) symmetry, and approximate molecular  $C_{2h}$  symmetry, and so has a perfectly staggered conformation around the central C–C bond and thus a Y–C–C–Y torsion angle of precisely  $180^\circ$ ; the structure closely resembles those of the two inequivalent molecules in the structure of the previously reported  $Y = ferrocenyl$  derivative, **1c<sub>2</sub>** [14], or the molecule in the structure **2<sub>2</sub>** [35], all three of which also have  $C_i$  symmetry. The other conformer present, although also staggered, has no crystallographic, or even approximate molecular,

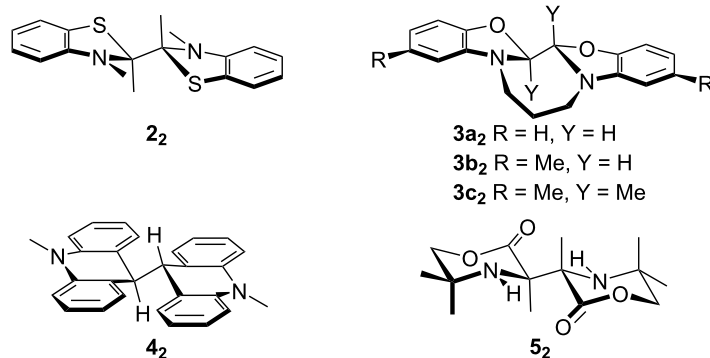
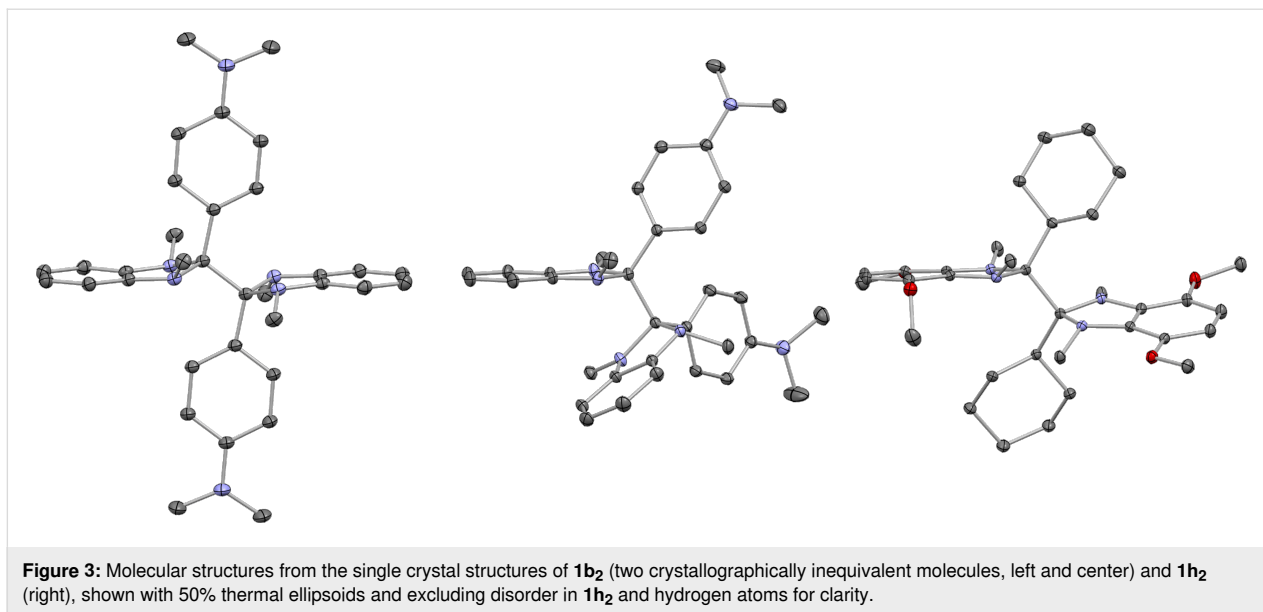


**Figure 2:** Crystallographically characterized molecules related to DMBI dimers.



symmetry and is characterized by a Y–C–Y torsion angle of  $60.3^\circ$ . The conformation found in the structure of the Y = cyclohexyl, R' = OMe derivative, **1h<sub>2</sub>** (Figure 3), is somewhat similar to that previously reported for its non-methoxylated analogue **1e<sub>2</sub>** [14]; the **1h<sub>2</sub>** molecule does not have the crystallographic  $C_2$  symmetry of the latter, but does have approximate molecular  $C_2$  symmetry, while the Y–C–Y torsion angles for **1h<sub>2</sub>** and **1e<sub>2</sub>** are  $149.4^\circ$  and  $140.3^\circ$ , respectively, and thus both intermediate between the perfectly staggered ( $180^\circ$  torsion) and neighboring eclipsed conformation ( $120^\circ$ ). The imidazole rings in the previously reported and present dimer structures are mostly somewhat folded towards a puckered envelope conformation, generally with the Y group in a pseudo-axial position and the 1,3-methyl groups and the central C–C bond in pseudo-equatorial positions, although for one of the monomers in the unsymmetrical conformer in the structure of (N-DMBI)<sub>2</sub>, **1b<sub>2</sub>**, the Y and central bond are pseudo-equatorial and pseudo-axial, respectively. However, this folding is generally much less pronounced than in **1H** derivatives (see below, Figure 4, and Table S2 in Supporting Information File 1) presumably since in the dimers both 2-substituents (Y and the other monomer unit) are fairly bulky, whereas in the hydrides there is a large difference in bulk between the hydridic H-atom and the Y-group and thus a strong preference for Y to occupy a pseudo-equatorial position.

As with other **1<sub>2</sub>** species [14] and related organic [35,37,38] and organometallic dimers [22,39–46], the central C–C bond of the present dimers are rather long compared to typical C–C bonds, although not remarkably so given that these are hexasubstituted ethane derivatives. Values of 1.5899(11) and 1.6194(8) Å are found for the symmetrical and unsymmetrical conformers of

**1b<sub>2</sub>**, respectively, while a value of 1.6299(13) Å is found for **1h<sub>2</sub>**; these may be compared to hexasubstituted central C–C bond length values of 1.595(5) and 1.601(5) Å for the two inequivalent molecules of the Y = Fc, R = R' = H derivative **1c<sub>2</sub>** [14], 1.640(4) Å for the Y = cyclohexyl, R = R' = H derivative **1e<sub>2</sub>** [14], 1.573 Å for **2<sub>2</sub>** [35], and 1.591 Å for **5<sub>2</sub>** [38], while (PhEt<sub>2</sub>C)<sub>2</sub>, a simple hexa-substituted ethane, exhibits a central C–C bond length of 1.635 Å [47]. The tetrasubstituted central C–C bond of **4<sub>2</sub>** is also rather long (1.58 Å) [37]. Bridged benzoxazoline dimers, **3<sub>2</sub>**, have, on the other hand, relatively short C–C central bonds, perhaps due to the influence of the propanediyl tether; the hexasubstituted bond of **3e<sub>2</sub>** is only 1.549(6) Å in length, while the tetrasubstituted bonds of **3a<sub>2</sub>** and **3b<sub>2</sub>** are even shorter [36].

The crystallographically determined central C–C bond lengths for **1b<sub>2</sub>** are shorter than that previously reported for the Y = cyclohexyl, R = R' = H derivative **1e<sub>2</sub>** (1.640(4) Å) [14], despite DFT calculations indicating that the former dimer is considerably more weakly bonded [8,14] and kinetic evidence for the “cleavage-first” mechanism occurring in doping reactions using **1b<sub>2</sub>** but not **1e<sub>2</sub>** (see below). We have previously noted a similar lack of correlation between bond length and bond dissociation energy in comparing the structures of **1c<sub>2</sub>** (Y = Fc; R = R' = H) and **1e<sub>2</sub>** (Y = cyclohexyl; R = R' = H) [14], and in comparing those of different organometallic dimers [22,46]. As noted in our previous work [14,22,46], the bond length depends on orbital overlap and steric strain in the dimer, whereas dissociation energetics also depend on the stability of the monomeric odd-electron species, which vary considerably; in the case of **1<sup>•</sup>** radicals an important factor is the ability of the Y substituent to delocalize spin density.

The **1H** structures (Figure 4) are similar to those of other DMBI-H structures in the literature [34,48–50] (and are compared in more detail in Supporting Information File 1, Table S2); in all cases the imidazole ring is folded in a “puckered envelope” conformation with the 2-Y and 1,3-dimethyl substituents in pseudo-equatorial positions and the reactive hydridic 2-H-atom pseudo-axial. The cation structures (Figure 5) give some insight into the variety of dopant-ion shapes and sizes that can be afforded by these types of dopants. The angle between the imidazolium ring and the aromatic ring of the **1g**<sup>+</sup>Γ<sup>−</sup> is 41.5°, close to the range of values previously reported for **1b**<sup>+</sup> salts (42.5–52.5°) [19,34] and for salts of Y = Ph, R = R' = H cations with different counterions (42.0–54.9°) [51–53]. As expected, owing to reduced steric interactions associated with the five-membered rather than six-membered aromatic ring, the structure of **1i**<sup>+</sup>PF<sub>6</sub><sup>−</sup> contains a somewhat more planar cation (31.9°). Finally, we note that the new structures reported here mean that the **1b** and **1h** systems join the **1c** (Y = Fc; R = R' = H) system [50] as families for which **1**<sup>+</sup>, **1H**, and **1**<sub>2</sub> members are all crystallographically characterized.

## Electrochemistry

The **1**<sup>+</sup>, **1H**, and **1**<sub>2</sub> species were investigated using cyclic voltammetry in THF/0.1 M Bu<sub>4</sub>NPF<sub>6</sub> at a scan rate of 50 mV s<sup>−1</sup>. The voltammograms (shown for one series of compounds in Figure 6) were qualitatively similar to those reported and shown

elsewhere for other compounds of the same classes [9,13,19,24], and the redox potentials are summarized in Table 1. The cations exhibit features assigned to  $E(\mathbf{1}^+/\mathbf{1}^\bullet)$  that are non-reversible owing to the rapid dimerization of **1**<sup>•</sup>. These values are important in determining the overall thermodynamic reducing power of the dimers according to:

$$E(\mathbf{1}^+/0.5\mathbf{1}_2) = E(\mathbf{1}^+/\mathbf{1}^\bullet) + \Delta G_{\text{diss}}(\mathbf{1}_2)/2F, \quad (1)$$

where  $\Delta G_{\text{diss}}(\mathbf{1}_2)$  is the free-energy change for dissociation of **1**<sub>2</sub> to **1**<sup>•</sup> (dissociation energetics are not estimated in the present work, but have been estimated using DFT calculations for **1b**–**e**<sub>2</sub> in previous works [8,14] and, in favorable cases, can be experimentally estimated using electron spin resonance [14] or using dissociation and dimerization barriers from reaction kinetics and variable scan-rate electrochemistry, respectively [54]) and where *F* is the Faraday constant. Similarly, at least for cases where the reactive hydrides of **1H** derivatives are ultimately lost as H<sub>2</sub>, the strength of **1H** dopants is given by:

$$E(\mathbf{1}^+, 0.5\text{H}_2/\mathbf{1H}) = E(\mathbf{1}^+/\mathbf{1}^\bullet) + \Delta G_{\text{diss}}(\mathbf{1H})/F - \Delta G_{\text{diss}}(\text{H}_2)/2F, \quad (2)$$

where  $\Delta G_{\text{diss}}(\mathbf{1H})$  is the free-energy change for dissociation of **1H** to **1**<sup>•</sup> and H<sup>•</sup> (again, not discussed in this work), and

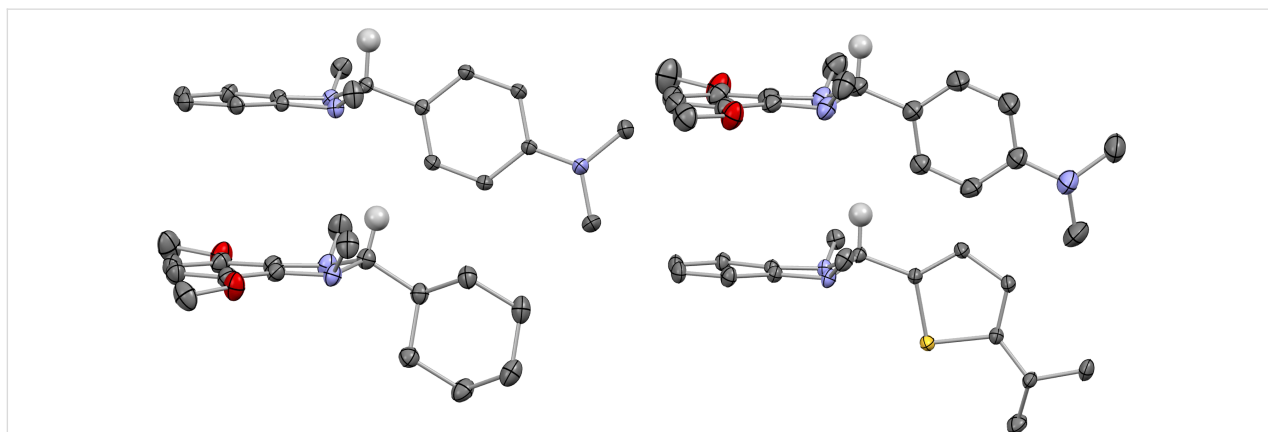


**Figure 4:** Molecular structures from the single crystal structures of **1bH** (upper left), **1gH** (upper right), **1hH** (lower left), and **1iH** (lower right), shown with 50% thermal ellipsoids and excluding hydrogen atoms for clarity, except for the hydridic 2-hydrogen atoms (located and refined for **1bH**, geometrically placed for the others).

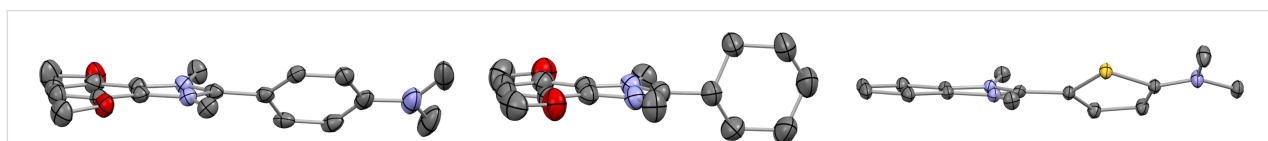


**Figure 5:** Structures of the cations from the single crystal structures of **1g**<sup>+</sup>Γ<sup>−</sup> (left), **1h**<sup>+</sup>PF<sub>6</sub><sup>−</sup> (center), and **1i**<sup>+</sup>PF<sub>6</sub><sup>−</sup> (right), shown with 50% thermal ellipsoids and excluding hydrogen atoms and counter anions.

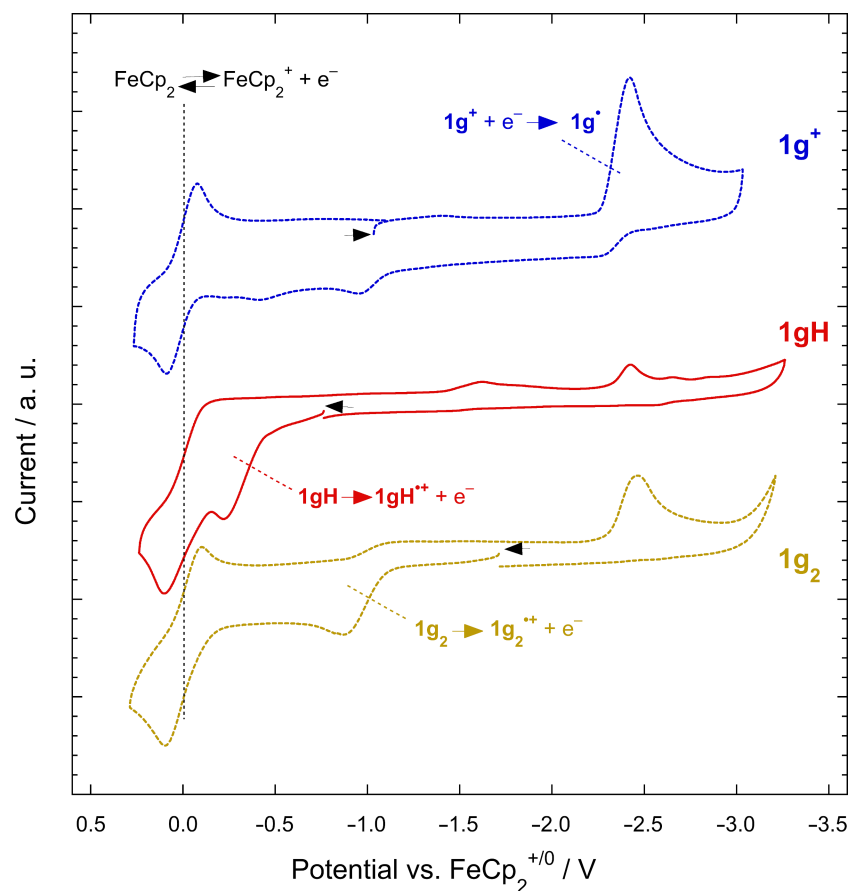


**Figure 6:** Cyclic voltammograms ( $50 \text{ mV s}^{-1}$ , THF,  $0.1 \text{ M Bu}_4\text{NPF}_6$ ) of  $1\mathbf{g}^+\text{PF}_6^-$ ,  $1\mathbf{gH}$ , and  $1\mathbf{g}_2$ , in each case containing ferrocene as an internal reference. Black arrows indicate the starting point and scan initial direction for each voltammograms. Note that the oxidation peak of  $1\mathbf{g}_2$  is seen in the voltammogram of  $1\mathbf{g}^+\text{PF}_6^-$  following scanning of the reduction peak, while the reduction peak of the cation is seen in the voltammograms of both  $1\mathbf{gH}$  and  $1\mathbf{g}_2$  following scanning of the irreversible oxidation peaks.

**Table 1:** Electrochemical potentials (V) for DMBI derivatives<sup>a</sup>.

	$E_{\text{red}}(1^+/1^\bullet)$	$E_{\text{ox}}(1\mathbf{H}^+/1\mathbf{H})$	$E_{\text{ox}}(1_2^+/1_2)$
<b>1b</b> (Y = C <sub>6</sub> H <sub>4</sub> -4-NMe <sub>2</sub> ; R = R' = H)	-2.38 <sup>b</sup>	-0.13 <sup>c</sup>	-0.75 <sup>b</sup>
<b>1c</b> (Y = Fc; R = R' = H)	-2.24 <sup>d</sup>	-0.06 <sup>e</sup>	-0.89 <sup>d</sup>
<b>1d</b> (Y = Rc; R = R' = H)	-2.29 <sup>d</sup>	-0.07 <sup>e</sup>	-0.59 <sup>d</sup>
<b>1e</b> (Y = cy-C <sub>6</sub> H <sub>11</sub> ; R = R' = H)	-2.45 <sup>d</sup>	-0.06	-0.64 <sup>d</sup>
<b>1g</b> (Y = C <sub>6</sub> H <sub>4</sub> -4-NMe <sub>2</sub> ; R = H; R' = OMe)	-2.42	-0.22	-0.87
<b>1h</b> (Y = cy-C <sub>6</sub> H <sub>11</sub> ; R = H; R' = OMe)	-2.56	-0.11	-0.92
<b>1i</b> (Y = 2-C <sub>4</sub> H <sub>3</sub> S-5-NMe <sub>2</sub> ; R = R' = H)	-2.05	-0.22	–

<sup>a</sup>vs FeCp<sub>2</sub><sup>+0</sup> in THF,  $0.1 \text{ M Bu}_4\text{NPF}_6$ ; <sup>b</sup>data from reference [19]; <sup>c</sup>data from reference [8]; <sup>d</sup>data from reference [14]; <sup>e</sup>data from reference [50].

$\Delta G_{\text{diss}}(\text{H}_2)$  the free-energy change for dissociation of dihydrogen. The values of  $E(1^+/1^\bullet)$  are also relevant to the kinetics of steps in doping reactions that involve  $1^\bullet$ , in particular for doping reactions in which the initial step is dimer dissociation and the second step is an electron transfer from  $1^\bullet$  to SC (or SC<sup>•-</sup>). The  $E(1^+/1^\bullet)$  potentials for the Y = 4-dimethylaminophenyl  $1\mathbf{b}^+/1\mathbf{b}^\bullet$

and  $1\mathbf{g}^+/1\mathbf{g}^\bullet$  systems are both somewhat less reducing than those for their Y = cyclohexyl counterparts,  $1\mathbf{e}^+/1\mathbf{e}^\bullet$  and  $1\mathbf{h}^+/1\mathbf{h}^\bullet$ , respectively. These differences are also similar to those previously seen in the comparison of Y = metallocenyl systems  $1\mathbf{c}^+/1\mathbf{c}^\bullet$  and  $1\mathbf{d}^+/1\mathbf{d}^\bullet$  with  $1\mathbf{e}^+/1\mathbf{e}^\bullet$  (and in the DFT-calculated ionization energies of  $1\mathbf{c}-\mathbf{e}^\bullet$ ) [14,50] and are perhaps surprising

since 4-(dimethylamino)phenyl and metallocenyl groups are  $\pi$ -donors, unlike cyclohexyl, and thus might be expected to be better able to stabilize an adjacent cation. However, aryl and metallocenyl substituents also stabilize adjacent radicals more effectively than alkyl groups and this effect is presumably dominant in the present case. The importance of radical stabilization may in part be because the positive charges in  $Y = H$  or alkyl  $1^+$  ions is already substantially stabilized by the aromaticity of the benzimidazolium ions, whereas the spin densities of the corresponding  $1^\bullet$  radicals are highly localized; indeed DFT calculations for the  $Y = \text{alkyl } 1e^\bullet$  derivative indicate spin density almost entirely on the 2-position of the five-membered ring, while for  $Y = \text{aryl}$  and metallocenyl examples  $1b^\bullet$ ,  $1c^\bullet$ , and  $1d^\bullet$  there is substantial spin delocalization onto the  $Y$ -substituents [14,55]. Different extents of deviation from planarity in cations and radicals, as well as inductive effects, may also play a role.

The  $1i^+/1i^\bullet$  ( $Y = 5$ -(dimethylamino)-2-thienyl;  $R = R' = H$ ) potential is less reducing than that of  $1b^+/1b^\bullet$  ( $Y = 4$ -dimethylaminophenyl;  $R = R' = H$ ). 5-(Dimethylamino)-2-thienyl is more strongly  $\pi$ -donating than 4-dimethylaminophenyl, at least according to NMR and DFT data for molecules in which the (hetero)aryl group is more or less coplanar with a  $\pi$ -acceptor [56], although some tabulated Swain–Lupton substituent constants do suggest phenyl can be a stronger  $\pi$ -donor than thienyl towards another aryl ring [57]. Presumably inductive effects destabilizing  $1i^+$ , different extents of planarization, and improved radical stabilization by the 5-(dimethylamino)-2-thienyl substituent play a role. As expected,  $R' = \text{OMe}$  groups on the six-membered benzimidazolium ring *do* have a net cation-stabilizing effect, resulting in  $1g^\bullet$  and  $1h^\bullet$  being more reducing monomers than their non-methoxylated analogues  $1b^\bullet$  and  $1e^\bullet$ , respectively.

Cyclic voltammograms of both  $1H$  and  $1_2$  both reveal irreversible oxidations (with the corresponding  $1^+$  reductions seen in subsequent reductive cycles, see Figure 6 for examples). These  $1H^{++}/1H$  and  $1_2^{++}/1_2$  potentials are relevant to the air stability of the hydrides and dimers, respectively, as well as to other processes in which  $1H$  or  $1_2$  acts as an electron donor, such as the initiation step proposed for the radical-chain dehalogenation of  $\alpha$ -dihaloketones by a  $1H$  derivative [58] and dimer n-doping reactions that proceed via the “ET-first” mechanism (see below). In all cases the dimers are more easily oxidized, consistent with their greater air sensitivity. The impact of the  $Y$ -substituents on both  $1H^{++}/1H$  and  $1_2^{++}/1_2$  potentials is not straightforward; one would expect  $\pi$ -conjugated substituents to make little contribution to the HOMO of either  $1H$  or  $1_2$  (as shown in calculated molecular orbitals for several examples [14,50,55,59,60]) and so the dependence of these potentials on

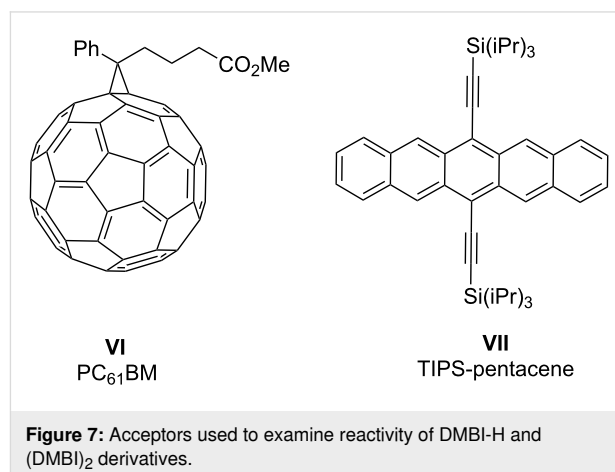
$Y$  is likely to be due to a combination of inductive effects and perhaps steric effects on the molecular conformation. As expected, methoxy  $R'$  substituents lead to  $1H^{++}/1H$  and  $1_2^{++}/1_2$  potentials that are more reducing than those for analogous species without these groups.  $1h_2$  ( $Y = \text{cyclohexyl}$ ,  $R = H$ ,  $R' = \text{MeO}$ ) is the most easily oxidized DMBI dimer that we have examined to date; however, it is a little less easily oxidized than  $[\text{RuCp}^*(1,3,5\text{-Me}_3\text{C}_6\text{H}_3)]_2$  ( $-1.09\text{ V}$ ) [61] and, like  $[\text{RuCp}^*(1,3,5\text{-Me}_3\text{C}_6\text{H}_3)]_2$ , can still be handled in air.

## Reactivity

To compare the reactivity of the new compounds towards relevant organic semiconductors (SC), we have examined the reactions of the  $1H$  derivatives with the solubilized fullerene  $\text{PC}_{61}\text{BM}$  (**VI**, Figure 7) and that of the  $1_2$  derivatives with 6,13-bis(triisopropylsilyl)ethynyl)pentacene (TIPS-pentacene, **VII**, Figure 7), since we have previously found that these dopant class/SC combinations often react on a timescale suitable for monitoring using UV–vis–NIR spectroscopy ( $1H$  derivatives do not react significantly with **VII** in solution at room temperature, while the reactions of  $1_2$  derivatives and **VI** are very rapid) [9,14,50,61]. Figure 8a compares the evolution of the absorbance at 1030 nm, corresponding to a  $\text{VI}^{\bullet-}$  absorption maximum, when doping excess **VI** with  $1H$  derivatives in chlorobenzene at 293 K in the absence of light, air, and water. In each case the reaction is apparently first order in dopant, consistent with the rate law:

$$d[\text{VI}^{\bullet-}] / dt = k[1H][\text{VI}] \quad (3)$$

previously demonstrated for  $1bH$  and **VI** [9]. The rate constants,  $k$ , obtained assuming this rate law are shown in Table 2 (the value for  $3b$  being similar to that previously determined [9]). One can anticipate, extending the Hammond postulate, that increased driving forces should correlate with reduced barriers





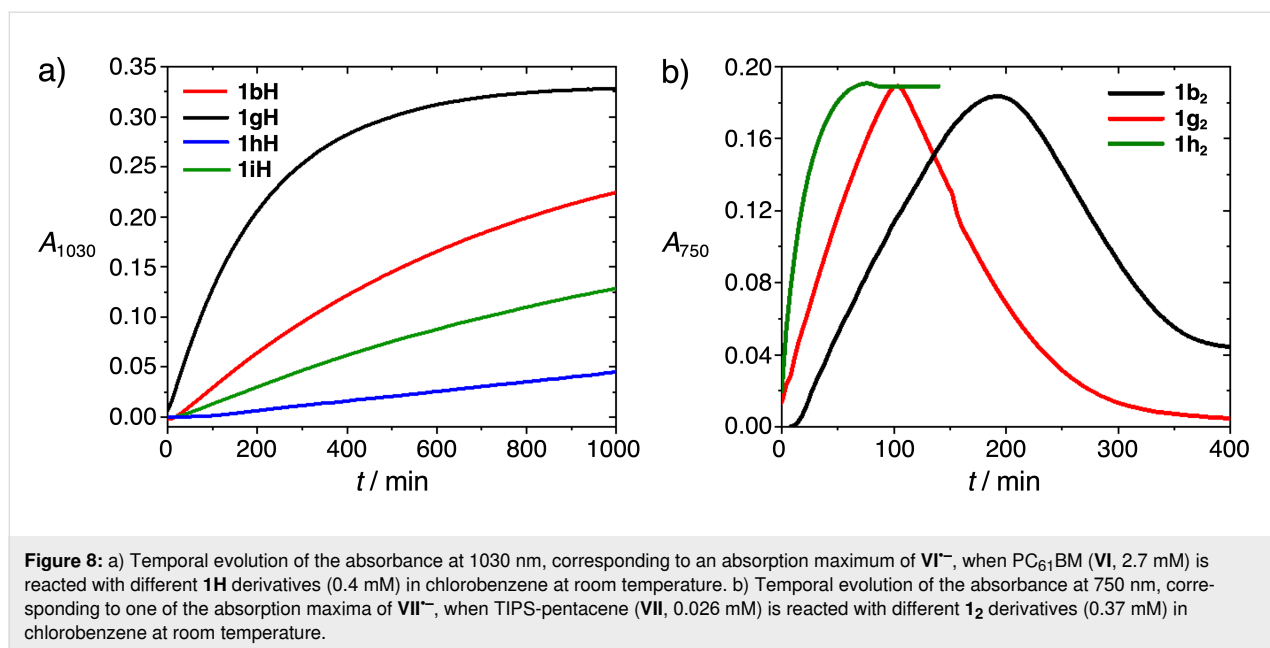


**Figure 8:** a) Temporal evolution of the absorbance at 1030 nm, corresponding to an absorption maximum of  $\text{VI}^{\cdot-}$ , when  $\text{PC}_{61}\text{BM}$  (**VI**, 2.7 mM) is reacted with different **1H** derivatives (0.4 mM) in chlorobenzene at room temperature. b) Temporal evolution of the absorbance at 750 nm, corresponding to one of the absorption maxima of  $\text{VII}^{\cdot-}$ , when TIPS-pentacene (**VII**, 0.026 mM) is reacted with different **1<sub>2</sub>** derivatives (0.37 mM) in chlorobenzene at room temperature.

**Table 2:** Rate constants for the reaction of DMBI-H derivatives and  $\text{PC}_{61}\text{BM}$ .

	$k$ [ $\text{M}^{-1} \text{min}^{-1}$ ]
<b>1bH</b> (Y = $\text{C}_6\text{H}_4$ -4- $\text{NMe}_2$ ; R = R' = H)	0.26
<b>1gH</b> (Y = $\text{C}_6\text{H}_4$ -4- $\text{NMe}_2$ ; R = H; R' = OMe)	0.48
<b>1hH</b> (Y = cy- $\text{C}_6\text{H}_{11}$ ; R = H; R' = OMe)	0.04
<b>1iH</b> (Y = 2- $\text{C}_4\text{H}_3\text{S}$ -5- $\text{NMe}_2$ ; R = R' = H)	0.13

and increased rate constants. Values of  $k$  do *not* correlate with the  $\text{1H}^{\cdot+}/\text{1H}$  potentials, but, at least when comparing aryl and alkyl Y substituents and when comparing R' = H and R' = OMe examples, do correlate with the expected stability of the resultant  $\text{1}^{\cdot+}$  cations, which is also expected to correlate with the hydride donor strength of **1H**. This is consistent with previous findings that the first and rate-determining step of several **1H**/SC reactions, including **1H**/**VI** reactions, is *not* an electron transfer, but a hydride transfer [8,9]. There is conflicting evidence in the literature regarding the  $\pi$ -donor characteristics of phenyl and thienyl groups [56,57], while thienyl is more inductively electron-withdrawing [57], as noted in the electrochemical section; however, the observed rate constants for **1bH** and **1iH** suggest that 5-dimethylamino-2-thienyl affords less net charge stabilization than 4-dimethylaminophenyl.

Two reaction pathways have been established for the oxidation of organometallic and organic dimers. A “cleavage-first” mechanism, whereby the dimer is in equilibrium with a small concentration of the corresponding odd-electron monomer, which can then rapidly react with an acceptor such as an organic semiconductor (SC) through an exergonic electron transfer (ET), has

been observed for the reactions of several relatively weakly bonded dimeric dopants (the Y = metallocenyl DMBI dimers **1c<sub>2</sub>** and **1d<sub>2</sub>** as well as various organometallic dimers) with **VII** [14,46,61], as well as in the oxidation of bis(3,5,5-trimethyl-2-morpholinon-3-yl), **5<sub>2</sub>** (Figure 2), by isatin derivatives [62]. In the alternative “ET-first” mechanism the first step is an endergonic dimer-to-SC ET; subsequent rapid cleavage of the odd-electron dimer cation affords the stable monomer cation and an odd-electron monomer, the latter then undergoing an exergonic ET to another SC molecule. The “ET-first” mechanism occurs in parallel with the “cleavage-first” mechanism for many of the **VII** doping reactions mentioned above and is the only mechanism seen for dimeric dopants that are more strongly bound (**1e<sub>2</sub>**, as well as various organometallic dimers including  $[\text{RuCp}^*(1,3,5\text{-Me}_3\text{C}_6\text{H}_3)_2]$  [14,46,61], as well as being observed in different contexts in, for example, the oxidation of **4<sub>2</sub>** by various quinone derivatives [63]. For both mechanisms, the first steps are typically rate determining and thus, in general, the rate law is:

$$d[\text{SC}^{\cdot-}]/dt = 2k_1[\mathbf{1}_2] + 2k_2[\mathbf{1}_2][\text{SC}], \quad (4)$$

where  $k_1$  and  $k_2$  are rate constants for the first steps of the “cleavage first” and “ET-first” pathways respectively,  $k_1$  being negligible in the case of strongly bound dimers.

Figure 8b compares the evolution of one of the distinctive  $\text{VII}^{\bullet-}$  absorptions when doping **VII** with excess  $\mathbf{1}_2$  derivatives in chlorobenzene at 293 K in the absence of light, air, and water. In the case of the  $Y = 4$ -dimethylaminophenyl dimers  $\mathbf{1b}_2$  and  $\mathbf{1g}_2$ , the  $\text{VII}^{\bullet-}$  absorption grows in and then falls approximately linearly at a comparable rate. This type of plot is a signature of dimer/**VII** combinations for which the “cleavage-first” pathway is important and has previously been seen for the reactions of **VII** with  $\mathbf{1c}_2$ ,  $\mathbf{1d}_2$ ,  $(\text{RhCp}^*\text{Cp})_2$ , and one of the isomers of  $[\text{RuCp}^*\{1,4-(\text{Me}_2\text{N})_2\text{C}_6\text{H}_4\}]_2$ , all of which are calculated to be relatively weakly bonded [14,46,61]. Specifically, this behavior is consistent with a “cleavage-first” mechanism in which the initial cleavage is rate determining and for which the resultant one-electron monomers are capable of reducing both **VII** to  $\text{VII}^{\bullet-}$  (−1.55 V) and  $\text{VII}^{\bullet-}$  to  $\text{VII}^{2-}$  (−1.93 V); since the cleavage is rate determining, **VII** will be converted to  $\text{VII}^{\bullet-}$  and then, when excess dimer is used, to  $\text{VII}^{2-}$  with a comparable rate constant. Indeed spectra obtained at long-reaction times (see Supporting Information File 1, Figure S7) are similar to those previously attributed to  $\text{VII}^{2-}$  [14,46,61], such as the reaction product of **VII** and Na:K. On the other hand, when *only* the “ET-first” mechanism is operative, the conversion of  $\text{VII}^{\bullet-}$  to  $\text{VII}^{2-}$  will be much slower, if it is even observable, than the initial formation of  $\text{VII}^{\bullet-}$  from **VII** due to the considerably greater endergonicity expected for this step. This is seen for the solution reaction of  $\mathbf{1h}_2$ , where, as in the case of non-methoxylated analogue  $\mathbf{1e}_2$ , only the formation of  $\text{VII}^{\bullet-}$  is seen and the growth in its absorbance can be fitted as first order in **VII**. Returning to the case of  $\mathbf{1b}_2$  and  $\mathbf{1g}_2$ , we note that the rise in  $\text{VII}^{\bullet-}$  absorption is neither zero-order nor first-order in **VII**, consistent with *both* mechanisms contributing, as previously demonstrated by more extensive investigations in the case of  $\mathbf{1c}_2$ ,  $\mathbf{1d}_2$ , and  $(\text{RhCp}^*\text{Cp})_2$  [14,61]. Thus, the  $Y = \text{alkyl}$  derivative ( $\mathbf{1h}_2$ , “ET-first” only) appears to be more strongly bonded than its  $Y = \text{aryl}$  counterparts ( $\mathbf{1b}_2$ ,  $\mathbf{1g}_2$ , both mechanisms), consistent with previous DFT calculations for  $\mathbf{1b}_2$  and  $\mathbf{1e}_2$  ( $\Delta U_{\text{diss}} = 163$  and  $210 \text{ kJ mol}^{-1}$ , respectively) and with the expected impact of the different  $Y$  substituents on monomer radical stability. In addition, the reaction of  $\mathbf{1h}_2$  and **VII** to form  $\text{VII}^{\bullet-}$  under the conditions used in the present study is complete much sooner than reactions using  $\mathbf{1b}_2$  or  $\mathbf{1g}_2$ , consistent with the ET-first reaction of  $\mathbf{3h}_2$  being more rapid than that for either  $\mathbf{1b}_2$  or  $\mathbf{1g}_2$ . Furthermore, the presumed “cleavage-first” reductions of  $\text{VII}^{\bullet-}$  to  $\text{VII}^{2-}$  proceed only slightly faster for  $\mathbf{1g}_2$  than for its non-methoxylated analogue  $\mathbf{1b}_2$ , suggesting the OMe groups only slightly weaken the bond in the latter and that the difference in the rates of formation of  $\text{VII}^{\bullet-}$  with these two

dimers is largely due to differences in the rate of the  $\mathbf{1}_2$ -to-**VII** ET reaction. Furthermore, the ordering of ET-first rates ( $\mathbf{1h}_2 > \mathbf{1g}_2 > \mathbf{1b}_2 > \mathbf{1e}_2$ , that for  $\mathbf{1e}_2$  being estimated by extrapolating previously reported parameters to the present conditions of temperature and concentration) reflecting the trend expected based on the  $E(\mathbf{1}_2^{\bullet+}/\mathbf{1}_2)$  values of Table 1.

It is worth noting that, although we see evidence for the “cleavage-first” mechanism in the reactions of  $\mathbf{1b}_2$  and  $\mathbf{1g}_2$  with **VII** at these specific concentrations, the “ET-first” mechanism will dominate these reactions (as well as those of the same dopants with more readily reduced SCs) under typical doping conditions, where SC and sub-stoichiometric dimer are mixed in solution prior to spin-coating at much higher concentrations. However, as we have previously noted, there are potential advantages and disadvantages for dimers for which the cleavage-first pathway is viable and those for which it is not. For the former class, doping in solution will proceed as long as  $E(\text{SC}/\text{SC}^{\bullet-})$  is less reducing than  $E(\mathbf{1}^{\bullet+}/0.5\mathbf{1}_2)$ , whereas in the latter this limit can only be reached as long as the  $\mathbf{1}_2$ -to-SC ET step is kinetically feasible under the reaction conditions. Moreover, for a given monomer redox potential,  $E(\mathbf{1}^{\bullet+}/\mathbf{1}^{\bullet})$ , a weakly bound dimer will be thermodynamically stronger (Equation 1) although, in some cases the effects of structural change on  $E(\mathbf{1}^{\bullet+}/\mathbf{1}^{\bullet})$  and  $\Delta G_{\text{diss}}(\mathbf{1}_2)$  partially cancel one another, as in the comparison of  $\mathbf{1b}_2$  vs  $\mathbf{1e}_2$  or  $\mathbf{1g}_2$  vs  $\mathbf{1h}_2$  (i.e., for  $Y = 4$ -dimethylaminophenyl, dimers are more weakly bound and monomers less reducing than for  $Y = \text{cyclohexyl}$ ). Conversely, the combination of a strongly bound dimer and an acceptor with  $E(\text{SC}/\text{SC}^{\bullet-})$  with the reach of  $E(\mathbf{1}^{\bullet+}/0.5\mathbf{1}_2)$ , but sufficiently cathodic that ET is very slow, could permit activation of doping by an external stimulus, such as photoexcitation, when desired, for example subsequent to processing.

## Conclusion

In conclusion we have reported a number of new DMBI-H and  $(\text{DMBI})_2$  reductants and compared their structures, electrochemistry, and reactivity with those of previously reported analogues. The structures show similar features to other related compounds, notably the dimers show long central C–C bonds. The  $E(\mathbf{1}^{\bullet+}/\mathbf{1}^{\bullet})$  potentials depend strongly on the 2-substituents ( $Y$ ), become increasing reducing (more negative) in the order  $Y = 5$ -(dimethylamino)thiophen-2-yl < 4-(dimethylamino)phenyl < cyclohexyl, indicating the effects of radical stabilization are more important than those of cation stabilization, while the  $E(\mathbf{1H}^{\bullet+}/\mathbf{1H})$  and  $E(\mathbf{1}_2^{\bullet+}/\mathbf{1}_2)$  potentials are less strongly and clearly affected by the 2-substituents. On the other hand, methoxy  $R'$  substituents lead to more reducing values of  $E(\mathbf{1}^{\bullet+}/\mathbf{1}^{\bullet})$ ,  $E(\mathbf{1H}^{\bullet+}/\mathbf{1H})$ , and  $E(\mathbf{1}_2^{\bullet+}/\mathbf{1}_2)$  than for  $R' = \text{H}$  analogues. The reaction rates of **1H** with  $\text{PC}_{61}\text{BM}$  (**VI**) increase in the order  $Y = \text{cyclohexyl} < 5$ -(dimethylamino)thiophen-2-yl < 4-(di-

methylamino)phenyl and  $R' = H < MeO$ , broadly consistent with the anticipated influence of these substituents on the DMBI<sup>+</sup> stability, as expected for a hydride-transfer reaction. The rates of reactions of the dimers with TIPS-pentacene (**VII**) follow a more complex pattern: examples with  $Y =$  cyclohexyl react solely via an “electron-transfer-first” mechanism, consistent with a relatively strongly bonded dimer, whereas  $Y =$  4-(dimethylamino)phenyl derivatives also react by a “cleavage-first” mechanism, consistent with a weaker central bond, which in turn is consistent with stabilization of the monomeric radicals by the 2-aryl substituents. The  $Y =$  cyclohexyl,  $R' = OMe$  dimer reacts most rapidly with TIPS-pentacene via the “ET-first” mechanism, consistent with this dimer also exhibiting the most cathodic value of  $E(I_2^{*+}/I_2)$ . Overall, this study gives insight into how substituents have different effects on the reactivity of DMBI-H derivatives and of (DMBI)<sub>2</sub> species, and may help provide guidance for dopant selection and for future dopant design.

## Supporting Information

### Supporting Information File 1

Synthetic and other experimental procedures, details of crystal-structure determinations, variable-temperature NMR data, stability data, optical spectra for reactivity studies, and NMR spectra of new compounds.

[<https://www.beilstein-journals.org/bjoc/content/supplementary/1860-5397-19-121-S1.pdf>]

## Acknowledgements

This work is partly based on the Ph.D. thesis of KAK [64].

## Funding

The work was primarily supported by the National Science Foundation through award DMR-1807797/2216857. Diffraction studies at New Mexico Highlands University were supported by the National Science Foundation’s PREM program through DMR-2122108. SJ was supported by Fulbright-Nehru Postdoctoral Fellowship from the United States-India Educational Foundation and Institute of International Education for (grant no. 2266/FNPDR/2017). This work was also authored in part by the National Renewable Energy Laboratory (NREL), operated by Alliance for Sustainable Energy, LLC, for the U.S. Department of Energy (DOE) under Contract No. DE-AC36-08GO28308; specifically, some of the data analysis was carried out as part of a Laboratory Directed Research and Development (LDRD) Program at NREL. The views expressed in the article do not necessarily represent the views of the DOE or the U.S. Government. The U.S. Government retains and the

publisher, by accepting the article for publication, acknowledges that the U.S. Government retains a nonexclusive, paid-up, irrevocable, worldwide license to publish or reproduce the published form of this work, or allow others to do so, for U.S. Government purposes.

## ORCID® iDs

Swagat K. Mohapatra - <https://orcid.org/0000-0002-4485-3967>

Georgii Bogdanov - <https://orcid.org/0000-0002-8655-3102>

Tatiana V. Timofeeva - <https://orcid.org/0000-0001-7475-3206>

Seth R. Marder - <https://orcid.org/0000-0001-6921-2536>

Stephen Barlow - <https://orcid.org/0000-0001-9059-9974>

## References

- Walzer, K.; Maennig, B.; Pfeiffer, M.; Leo, K. *Chem. Rev.* **2007**, *107*, 1233–1271. doi:10.1021/cr050156n
- Russ, B.; Glauddell, A.; Urban, J. J.; Chabinyk, M. L.; Segalman, R. A. *Nat. Rev. Mater.* **2016**, *1*, 16050. doi:10.1038/natrevmats.2016.50
- Lüsse, B.; Keum, C.-M.; Kasemann, D.; Naab, B.; Bao, Z.; Leo, K. *Chem. Rev.* **2016**, *116*, 13714–13751. doi:10.1021/acs.chemrev.6b00329
- Wang, Z.-K.; Liao, L.-S. *Adv. Opt. Mater.* **2018**, *6*, 1800276. doi:10.1002/adom.201800276
- Barlow, S.; Marder, S. R.; Lin, X.; Zhang, F.; Kahn, A. *Electrical Doping of Organic Semiconductors with Molecular Oxidants and Reductants. In Conjugated Polymers*, 4th ed.; Skotheim, T. A.; Reynolds, J.; Thompson, B. C., Eds.; CRC Press: Boca Raton, FL, USA, 2019. doi:10.1201/9780429190520-2
- Wahl, H. *Bull. Soc. Chim. Fr.* **1954**, 251–253.
- Wei, P.; Oh, J. H.; Dong, G.; Bao, Z. *J. Am. Chem. Soc.* **2010**, *132*, 8852–8853. doi:10.1021/ja103173m
- Jhulki, S.; Un, H.-I.; Ding, Y.-F.; Risko, C.; Mohapatra, S. K.; Pei, J.; Barlow, S.; Marder, S. R. *Chem* **2021**, *7*, 1050–1065. doi:10.1016/j.chempr.2021.01.020
- Naab, B. D.; Guo, S.; Olthof, S.; Evans, E. G. B.; Wei, P.; Millhauser, G. L.; Kahn, A.; Barlow, S.; Marder, S. R.; Bao, Z. *J. Am. Chem. Soc.* **2013**, *135*, 15018–15025. doi:10.1021/ja403906d
- Guo, H.; Yang, C.-Y.; Zhang, X.; Motta, A.; Feng, K.; Xia, Y.; Shi, Y.; Wu, Z.; Yang, K.; Chen, J.; Liao, Q.; Tang, Y.; Sun, H.; Woo, H. Y.; Fabiano, S.; Facchetti, A.; Guo, X. *Nature* **2021**, *599*, 67–73. doi:10.1038/s41586-021-03942-0
- Pallini, F.; Mattiello, S.; Manfredi, N.; Mecca, S.; Fedorov, A.; Sassi, M.; Al Kurdi, K.; Ding, Y.-F.; Pan, C.-K.; Pei, J.; Barlow, S.; Marder, S. R.; Nguyen, T.-Q.; Beverina, L. *J. Mater. Chem. A* **2023**, *11*, 8192–8201. doi:10.1039/d3ta00231d
- Ludvík, J.; Pragst, F.; Volke, J. *J. Electroanal. Chem. Interfacial Electrochem.* **1984**, *180*, 141–156. doi:10.1016/0368-1874(84)83576-5
- Naab, B. D.; Zhang, S.; Vandewal, K.; Salleo, A.; Barlow, S.; Marder, S. R.; Bao, Z. *Adv. Mater. (Weinheim, Ger.)* **2014**, *26*, 4268–4272. doi:10.1002/adma.201400668
- Zhang, S.; Naab, B. D.; Jucov, E. V.; Parkin, S.; Evans, E. G. B.; Millhauser, G. L.; Timofeeva, T. V.; Risko, C.; Brédas, J.-L.; Bao, Z.; Barlow, S.; Marder, S. R. *Chem. – Eur. J.* **2015**, *21*, 10878–10885. doi:10.1002/chem.201500611
- Naab, B. D.; Gu, X.; Kurosawa, T.; To, J. W. F.; Salleo, A.; Bao, Z. *Adv. Electron. Mater.* **2016**, *2*, 1600004. doi:10.1002/aelm.201600004

16. Yuan, D.; Huang, D.; Zhang, C.; Zou, Y.; Di, C.-a.; Zhu, X.; Zhu, D. *ACS Appl. Mater. Interfaces* **2017**, *9*, 28795–28801. doi:10.1021/acsami.7b07282
17. Schwarze, M.; Gaul, C.; Scholz, R.; Bussolotti, F.; Hofacker, A.; Schellhammer, K. S.; Nell, B.; Naab, B. D.; Bao, Z.; Spoltore, D.; Vandewal, K.; Widmer, J.; Kera, S.; Ueno, N.; Ortmann, F.; Leo, K. *Nat. Mater.* **2019**, *18*, 242–248. doi:10.1038/s41563-018-0277-0
18. Al Kurdi, K.; Gregory, S. A.; Jhulki, S.; Conte, M.; Barlow, S.; Yee, S. K.; Marder, S. R. *Mater. Adv.* **2020**, *1*, 1829–1834. doi:10.1039/d0ma00406e
19. Un, H.-I.; Gregory, S. A.; Mohapatra, S. K.; Xiong, M.; Longhi, E.; Lu, Y.; Rigin, S.; Jhulki, S.; Yang, C.-Y.; Timofeeva, T. V.; Wang, J.-Y.; Yee, S. K.; Barlow, S.; Marder, S. R.; Pei, J. *Adv. Energy Mater.* **2019**, *9*, 1900817. doi:10.1002/aenm.201900817
20. Lungwitz, D.; Joy, S.; Mansour, A. E.; Opitz, A.; Karunasena, C.; Li, H.; Panjwani, N. A.; Moudgil, K.; Tang, K.; Behrends, J.; Barlow, S.; Marder, S. R.; Brédas, J.-L.; Graham, K.; Koch, N.; Kahn, A. *J. Phys. Chem. Lett.* **2023**, *14*, 5633–5640. doi:10.1021/acs.jpcclett.3c01022
21. Guo, S.; Kim, S. B.; Mohapatra, S. K.; Qi, Y.; Sajoto, T.; Kahn, A.; Marder, S. R.; Barlow, S. *Adv. Mater. (Weinheim, Ger.)* **2012**, *24*, 699–703. doi:10.1002/adma.201103238
22. Mohapatra, S. K.; Fonari, A.; Risko, C.; Yesudas, K.; Moudgil, K.; Delcamp, J. H.; Timofeeva, T. V.; Brédas, J.-L.; Marder, S. R.; Barlow, S. *Chem. – Eur. J.* **2014**, *20*, 15385–15394. doi:10.1002/chem.201404007
23. Mohapatra, S. K.; Marder, S. R.; Barlow, S. *Acc. Chem. Res.* **2022**, *55*, 319–332. doi:10.1021/acs.accounts.1c00612
24. Zhu, X.-Q.; Zhang, M.-T.; Yu, A.; Wang, C.-H.; Cheng, J.-P. *J. Am. Chem. Soc.* **2008**, *130*, 2501–2516. doi:10.1021/ja075523m
25. Kūčkūkbay, H.; Çetinkaya, E.; Çetinkaya, B.; Lappert, M. F. *Synth. Commun.* **1997**, *27*, 4059–4066. doi:10.1080/00397919708005451
26. Pham, P. H.; Barlow, S.; Marder, S. R.; Luca, O. R. *Chem Catal.* **2023**, *3*, 100675. doi:10.1016/j.checat.2023.100675
27. Pallini, F.; Mattiello, S.; Cassinelli, M.; Rossi, P.; Mecca, S.; Tan, W. L.; Sassi, M.; Lanzani, G.; McNeill, C. R.; Caironi, M.; Beverina, L. *ACS Appl. Energy Mater.* **2022**, *5*, 2421–2429. doi:10.1021/acsaem.1c03893
28. Lim, C.-H.; Ilic, S.; Alherz, A.; Worrell, B. T.; Bacon, S. S.; Hynes, J. T.; Glusac, K. D.; Musgrave, C. B. *J. Am. Chem. Soc.* **2019**, *141*, 272–280. doi:10.1021/jacs.8b09653
29. Ghosh, R.; Kushwaha, A.; Das, D. *J. Phys. Chem. B* **2017**, *121*, 8786–8794. doi:10.1021/acs.jpcc.7b05947
30. Crippa, G. B.; Maffei, S. *Gazz. Chim. Ital.* **1941**, *71*, 194–200.
31. Balachandran, K. S.; George, M. V. *Indian J. Chem.* **1973**, *11*, 1267–1271.
32. Speier, G.; Párkányi, L. *J. Org. Chem.* **1986**, *51*, 218–221. doi:10.1021/jo00352a016
33. Reddy, A. P. R.; Veeranagaiah, V.; Ratnam, C. V. *Indian J. Chem.* **1985**, *B24*, 367–371.
34. Bardagot, O.; Aumaître, C.; Monmagnon, A.; Pécaut, J.; Bayle, P.-A.; Demadrille, R. *Appl. Phys. Lett.* **2021**, *118*, 203904. doi:10.1063/5.0047637
35. Miller-Srenger, E. *Acta Crystallogr., Sect. B: Struct. Crystallogr. Cryst. Chem.* **1973**, *29*, 1119–1124. doi:10.1107/s0567740873003973
36. Ramirez-Montes, P. I.; Ochoa, M. E.; Rodríguez, V.; Santillan, R.; García-Ortega, H.; Rodríguez, P.; Farfán, N. *Tetrahedron Lett.* **2012**, *53*, 5887–5890. doi:10.1016/j.tetlet.2012.08.094
37. Preuss, J.; Zanker, V.; Gieren, A. *Acta Crystallogr., Sect. B: Struct. Crystallogr. Cryst. Chem.* **1977**, *33*, 2317–2319. doi:10.1107/s0567740877008346
38. Haltiwanger, R. C.; Koch, T. H.; Olesen, J. A.; Kim, C. S.; Kim, N. K. *J. Am. Chem. Soc.* **1977**, *99*, 6327–6331. doi:10.1021/ja00461a026
39. Andrianov, V. G.; Struchkov, Y. T.; Petrakova, V. A.; Vol'kenau, N. A. *Koord. Khim.* **1986**, *12*, 978–980.
40. Gaudet, M. V.; Hanson, A. W.; White, P. S.; Zaworotko, M. J. *Organometallics* **1989**, *8*, 286–293. doi:10.1021/om00104a004
41. Lee, S.; Lovelace, S. R.; Arford, D. J.; Geib, S. J.; Weber, S. G.; Cooper, N. J. *J. Am. Chem. Soc.* **1996**, *118*, 4190–4191. doi:10.1021/ja952217c
42. Hsu, S. C. N.; Yeh, W.-Y.; Lee, G.-H.; Peng, S.-M. *J. Am. Chem. Soc.* **1998**, *120*, 13250–13251. doi:10.1021/ja982773h
43. Hitchcock, P. B.; Lappert, M. F.; Protchenko, A. V. *J. Am. Chem. Soc.* **2001**, *123*, 189–190. doi:10.1021/ja005580e
44. Shao, L.; Geib, S. J.; Badger, P. D.; Cooper, N. J. *J. Am. Chem. Soc.* **2002**, *124*, 14812–14813. doi:10.1021/ja027081e
45. Tamm, M.; Bannenberg, T.; Fröhlich, R.; Grimme, S.; Gerenkamp, M. *Dalton Trans.* **2004**, 482–491. doi:10.1039/b314347c
46. Longhi, E.; Risko, C.; Bacsá, J.; Khrustalev, V.; Rigin, S.; Moudgil, K.; Timofeeva, T. V.; Marder, S. R.; Barlow, S. *Dalton Trans.* **2021**, *50*, 13020–13030. doi:10.1039/d1dt02155a
47. Kratt, G.; Beckhaus, H.-D.; Lindner, H. J.; Rüdhardt, C. *Chem. Ber.* **1983**, *116*, 3235–3263. doi:10.1002/cber.19831160921
48. Beauchamp, A. L.; Montgrain, F.; Wuest, J. D. *Acta Crystallogr., Sect. C: Cryst. Struct. Commun.* **1987**, *43*, 1557–1560. doi:10.1107/s0108270187091108
49. Mas-Marzá, E.; Poyatos, M.; Sanaú, M.; Peris, E. *Inorg. Chem.* **2004**, *43*, 2213–2219. doi:10.1021/ic035317p
50. Zhang, S.; Moudgil, K.; Jucov, E.; Risko, C.; Timofeeva, T. V.; Marder, S. R.; Barlow, S. *Inorg. Chim. Acta* **2019**, *489*, 67–77. doi:10.1016/j.ica.2019.02.003
51. Wright, A. G.; Weissbach, T.; Holdcroft, S. *Angew. Chem., Int. Ed.* **2016**, *55*, 4818–4821. doi:10.1002/anie.201511184
52. Mehrotra, S.; Raje, S.; Jain, A. K.; Angamuthu, R. *ACS Sustainable Chem. Eng.* **2017**, *5*, 6322–6328. doi:10.1021/acssuschemeng.7b01495
53. Li, X.; Hao, P.; Shen, J.; Fu, Y. *Dalton Trans.* **2018**, *47*, 6031–6035. doi:10.1039/c8dt00829a
54. Moudgil, K.; Mann, M. A.; Risko, C.; Bottomley, L. A.; Marder, S. R.; Barlow, S. *Organometallics* **2015**, *34*, 3706–3712. doi:10.1021/acs.organomet.5b00327
55. Uebe, M.; Yoshihashi, Y.; Noda, K.; Matsubara, M.; Ito, A. *J. Mater. Chem. C* **2018**, *6*, 6429–6439. doi:10.1039/c8tc01280f
56. Kwon, O.; Barlow, S.; Odom, S. A.; Beverina, L.; Thompson, N. J.; Zojer, E.; Brédas, J.-L.; Marder, S. R. *J. Phys. Chem. A* **2005**, *109*, 9346–9352. doi:10.1021/jp054334s
57. Hansch, C.; Leo, A.; Taft, R. W. *Chem. Rev.* **1991**, *91*, 165–195. doi:10.1021/cr00002a004
58. Tanner, D. D.; Chen, J. J. *J. Org. Chem.* **1989**, *54*, 3842–3846. doi:10.1021/jo00277a020
59. Riera-Galindo, S.; Orbelli Biroli, A.; Forni, A.; Puttisong, Y.; Tessore, F.; Pizzotti, M.; Pavlopoulou, E.; Solano, E.; Wang, S.; Wang, G.; Ruoko, T.-P.; Chen, W. M.; Kemerink, M.; Berggren, M.; di Carlo, G.; Fabiano, S. *ACS Appl. Mater. Interfaces* **2019**, *11*, 37981–37990. doi:10.1021/acsami.9b12441
60. Zeng, Y.; Zheng, W.; Guo, Y.; Han, G.; Yi, Y. *J. Mater. Chem. A* **2020**, *8*, 8323–8328. doi:10.1039/d0ta01087a

61. Guo, S.; Mohapatra, S. K.; Romanov, A.; Timofeeva, T. V.; Hardcastle, K. I.; Yesudas, K.; Risko, C.; Brédas, J.-L.; Marder, S. R.; Barlow, S. *Chem. – Eur. J.* **2012**, *18*, 14760–14772. doi:10.1002/chem.201202591
62. Bennett, R. W.; Wharry, D. L.; Koch, T. H. *J. Am. Chem. Soc.* **1980**, *102*, 2345–2349. doi:10.1021/ja00527a036
63. Colter, A. K.; Lai, C. C.; Parsons, A. G.; Ramsey, N. B.; Saito, G. *Can. J. Chem.* **1985**, *63*, 445–451. doi:10.1139/v85-073
64. Al Kurdi, K. Investigating Charge Transport in Conjugated Organic Materials. Ph.D. Thesis, Georgia Institute of Technology, Atlanta, GA, USA, 2021.

## License and Terms

This is an open access article licensed under the terms of the Beilstein-Institut Open Access License Agreement (<https://www.beilstein-journals.org/bjoc/terms>), which is identical to the Creative Commons Attribution 4.0 International License (<https://creativecommons.org/licenses/by/4.0>). The reuse of material under this license requires that the author(s), source and license are credited. Third-party material in this article could be subject to other licenses (typically indicated in the credit line), and in this case, users are required to obtain permission from the license holder to reuse the material.

The definitive version of this article is the electronic one which can be found at:  
<https://doi.org/10.3762/bjoc.19.121>